"The role of microRNA in CLL pathogenesis"

Carlo M. Croce, M.D.

The Ohio State University
Distinguished University Professor
The John W. Wolfe Chair in Human Cancer Genetics
Director, Institute of Genetics
Director, Human Cancer Genetics Program

Occurrence of the most frequent and recurrent chromosomal abnormalities in human CLL

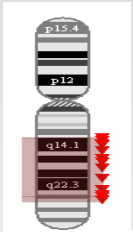

11q23

18 %

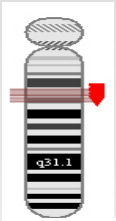

13q14

55 %

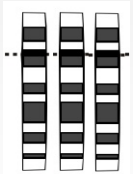

Trisomy 12

12 %

17p13

7%

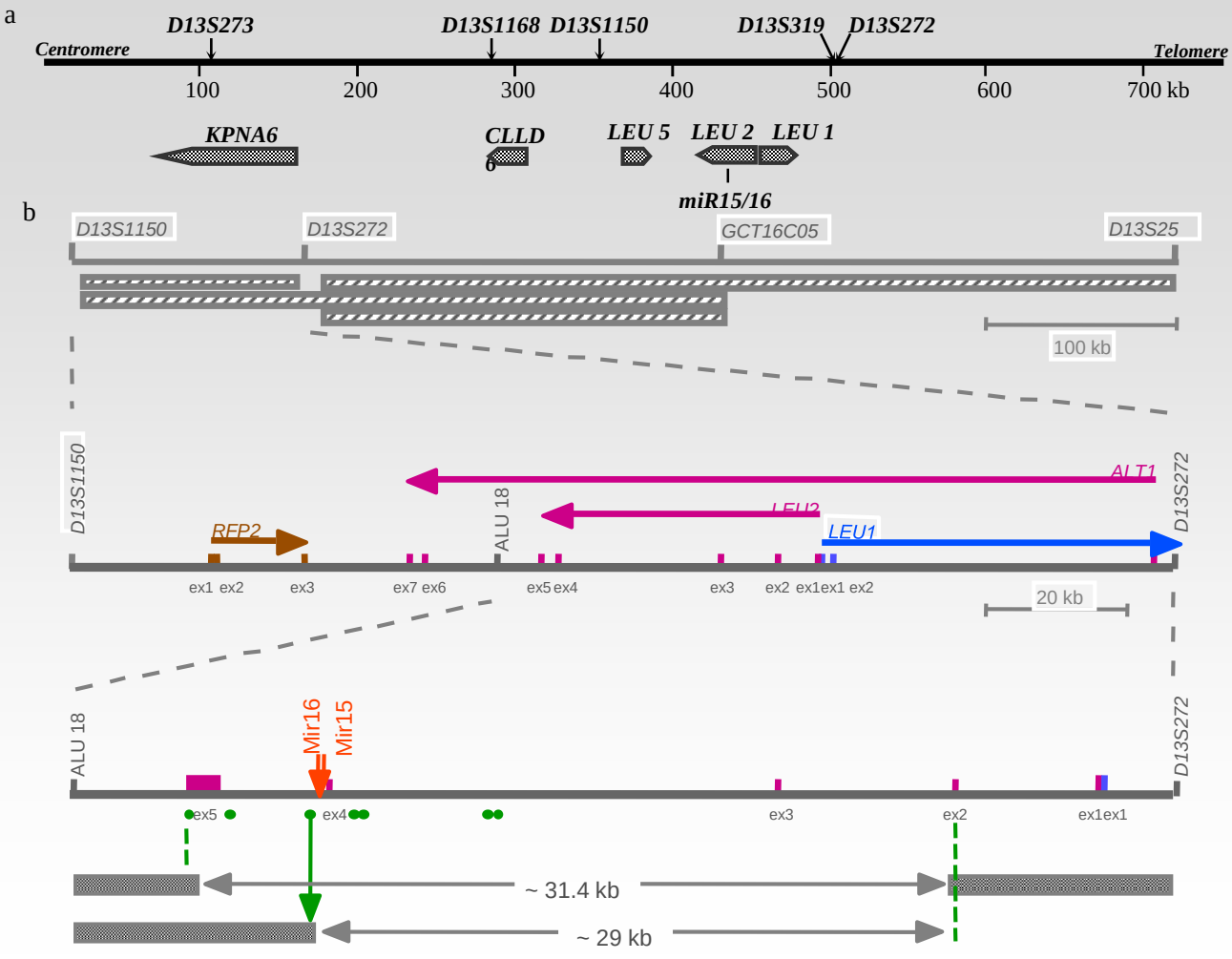
a
D13S273
D13S1168
D13S1150
D13S319
D13S272
Centromere
Telomere
100
200
300
400
500
600
700 kb
KPNA6
CLLD 6
LEU 5
LEU 2
LEU 1
miR15/16
b
D13S1150
D13S272
GCT16C05
D13S25
100 kb
D13S1150
ALT1
LEU2
LEU1
REP2
ALU 18
D13S272
ex1 ex2
ex3
ex7 ex6
ex5 ex4
ex3
ex2 ex1ex1 ex2
20 kb
ALU 18
Mir16
Mir15
D13S272
ex5
ex4
ex3
ex2
ex1ex1
~ 31.4 kb
~ 29 kb

Genetic variations in the genomic sequences of miRNAs in CLL patients *.

miRNA	Location **	CLL	Normals	miRNACHIP expression	Observation
miR-16-1	Germline pri-miRNA (CtoT)+7bp in 3'	2/75	0/160	Reduced to 15% and 40% of normal, respectively	Normal allele deleted in CLL cells in both patients (FISH, LOH); For one patient: Previous breast cancer; Mother died with CLL; sister died with breast ca;
miR-27b	Germline pri-miRNA (GtoA)+50bp in 3'	1/75	0/160	Normal	Mother throat and lung cancer at 58. Father lung cancer at 57.
miR-29b-2	pri-miRNA (GtoT)+212 in 3'	1/75	0/160	Reduced to 75%	Sister breast cancer at 88 (still living). Brother "some type of blood cancer" at 70.
miR-29b-2	pri-miRNAs ins (+A)+107 in 3'	3/75	0/160	Reduced to 80%	For two patients: Fam history of unspecified cancer
miR-187	pri-miRNA (TtoC)+73 in	1/75	0/160	NA	Unknown
miR-206	pre-miRNA 49(GtoT)	2/75	0/160	Reduced to 25%	Prostate cancer; mother esophogeal cancer. Brother prostate cancer sister breast cancer
miR-206	Somatic pri-miRNA (AtoT)-116 in 5'	1/75	0/160	Reduced to 25% (data only for one pt)	Aunt some type of leukemia (dead)
miR-29c	pri-miRNA (GtoA)31 in 5'	2/75	1/160	NA	Paternal grandmother CLL; sister breast ca. (one pt).
miR-122a	pre-miRNA 53(CtoT)	1/75	2/160	Reduced to 33%	Paternal uncle colon cancer.
miR-187	pre-miRNA 34(GtoA)	1/75	1/160	NA	Grandfather polycythemia vera. Father a history of cancer but not lymphoma.

Note: * - For each patient/normal control more than 12kb of genomic DNAs was sequenced and, in total, we screened by direct sequencing ~627kb of tumor DNA and about 700kb of normal DNA. The position of the mutations are reported in respect with the precursor miRNA molecule. The list of 42 microRNAs analyzed includes 15 members of the specific signature or members of the same clusters, *miR-15a, miR-16-1, miR-23a, miR-23b, miR-24-1, miR-24-2, miR-27a, miR-27b, miR-29b-2, miR-29c, miR-146, miR-155, miR-221, miR-222, miR-223* and 27 other microRNAs (randomly selected): *let-7a2, let-7b, miR-17-3p, miR-17-5p, miR-18, miR-19a, miR-19b-1, miR-20, miR-21, miR-30b, miR-30c-1, miR-30d, miR-30e, miR-32, miR-100, miR-105-1, miR-108, miR-122, miR-125b-1, miR-142-5p, miR-142-3p, miR-193, miR-181a, miR-187, miR-206, miR-224, miR-346.*

** - When normal correspondent DNA from bucal mucosa was available, the alteration was identified as germline when present or somatic when absent, respectively. FISH = fluorescence *in situ* hybridization; LOH = loss of heterozygosity; NA = not available

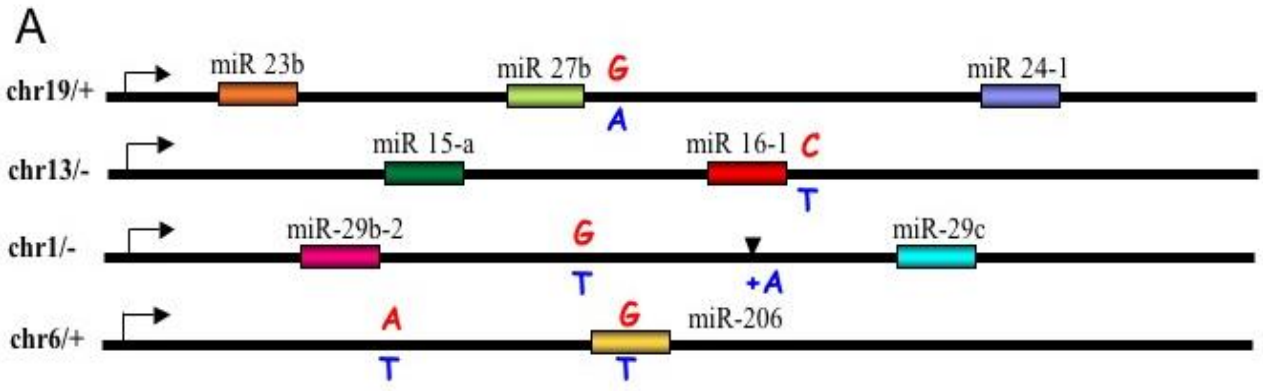
A
chr19/+
miR 23b
miR 27b
G
A
miR 24-1
chr13/-
miR 15-a
miR 16-1
C
T
chr1/-
miR-29b-2
G
T
+A
miR-29c
chr6/+
A
T
G
T
miR-206

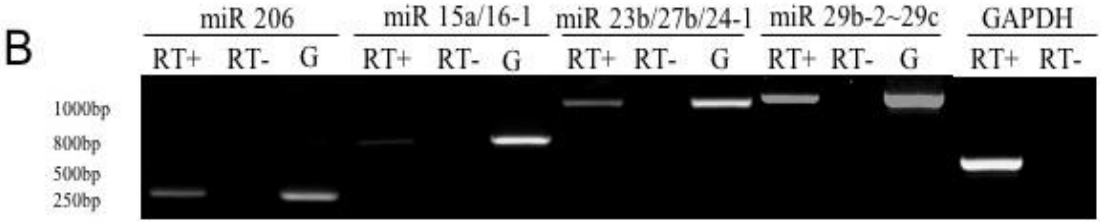
B
miR 206
miR 15a/16-1
miR 23b/27b/24-1
miR 29b-2~29c
GAPDH
RT+ RT- G RT+ RT- G RT+ RT- G RT+ RT- G RT+ RT-
1000bp
800bp
500bp
250bp

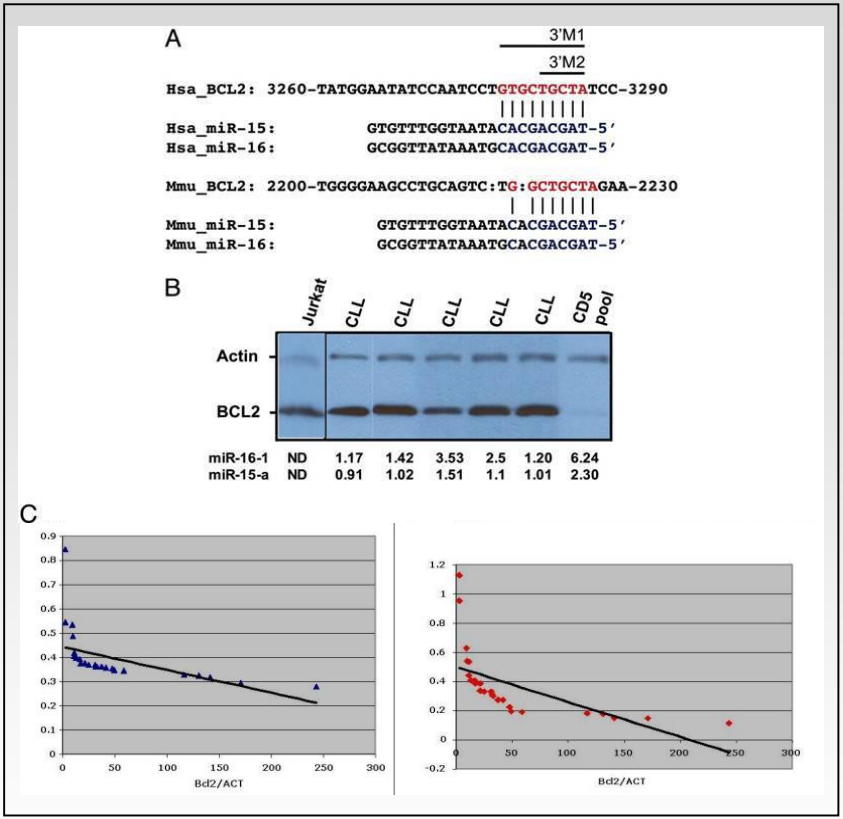

Bcl2 protein expression is inversely correlated with *miR-15a* and *miR-16-1* miRNAs expression in CLL patients. (*A*) The unique site of complementarity miR::mRNA is conserved in human and mouse and is the same for all four human m protein are inversely correlated with *miR-15a* and *miR-16-1* expression. Five different CLL cases are presented, and the normal cells were pools of $CD5^+$ B lymphocytes. The T cell leukemia Jurkat was used as control for Bcl2 protein expression. For normalization we used β-actin. The numbers represent normalized expression on miRNACHIP. ND, not determined. (*C*) The inverse correlation in the full set of 26 samples of CLL between miR-15a / miR-16-1 and Bcl2 protein expressions. The normalized Bcl2 expression is on abscissa vs. *miR-15a* (*Left*) and *miR-16-1* (*Right*) levels by miRNA chip on ordinates. ACT, β-actin.

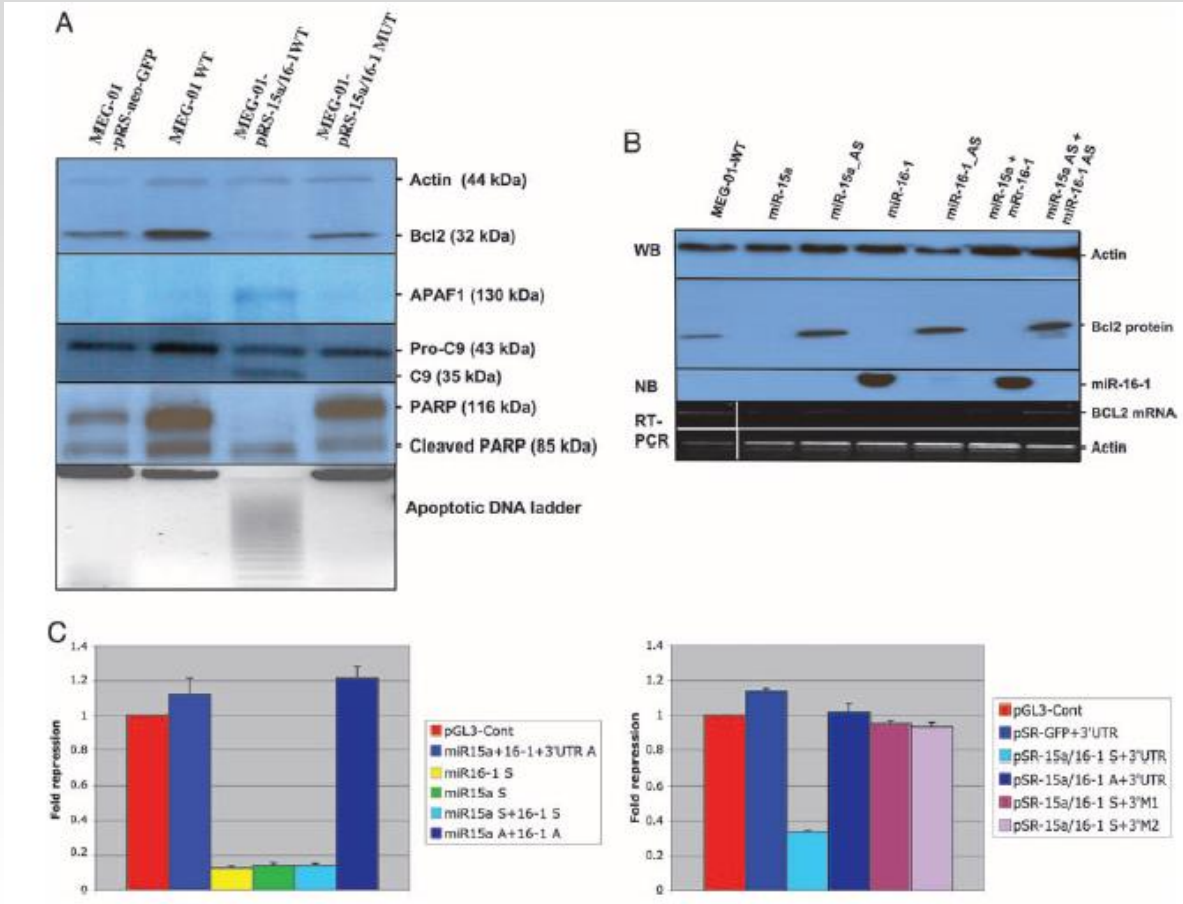
A
MEG-01 pRS-neo-GFP
MEG-01 WT
MEG-01-pRS-15a/16-1WT
MEG-01-pRS-15a/16-1 MUT
Actin (44 kDa)
Bcl2 (32 kDa)
APAF1 (130 kDa)
Pro-C9 (43 kDa)
C9 (35 kDa)
PARP (116 kDa)
Cleaved PARP (85 kDa)
Apoptotic DNA ladder
B
MEG-01-WT
miR-15a
miR-15a_AS
miR-16-1
miR-16-1_AS
miR-15a + miR-16-1
miR-15a AS + miR-16-1 AS
WB
Actin
Bcl2 protein
NB
miR-16-1
RT-PCR
BCL2 mRNA
Actin
C
Fold repression
pGL3-Cont
miR15a+16-1+3'UTR A
miR16-1 S
miR15a S
miR15a S+16-1 S
miR15a A+16-1 A
Fold repression
pGL3-Cont
pSR-GFP+3'UTR
pSR-15a/16-1 S+3'UTR
pSR-15a/16-1 A+3'UTR
pSR-15a/16-1 S+3'M1
pSR-15a/16-1 S+3'M2

nature medicine

ABT-199, a potent and selective BCL-2 inhibitor, achieves antitumor activity while sparing platelets

Andrew J Souers[1], Joel D Leverson[1], Erwin R Boghaert[1], Scott L Ackler[1], Nathaniel D Catron[1], Jun Chen[1], Brian D Dayton[1], Hong Ding[1], Sari H Enschede[1], Wayne J Fairbrother[2], David C S Huang[3,4], Sarah G Hymowitz[2], Sha Jin[1], Seong Lin Khaw[3,4], Peter J Kovar[1], Lloyd T Lam[1], Jackie Lee[2], Heather L Maecker[2], Kennan C Marsh[1], Kylie D Mason[3–5], Michael J Mitten[1], Paul M Nimmer[1], Anatol Oleksijew[1], Chang H Park[1], Cheol-Min Park[1,7], Darren C Phillips[1], Andrew W Roberts[3–5], Deepak Sampath[2], John F Seymour[4,6], Morey L Smith[1], Gerard M Sullivan[1], Stephen K Tahir[1], Chris Tse[1], Michael D Wendt[1], Yu Xiao[1], John C Xue[1], Haichao Zhang[1], Rod A Humerickhouse[1], Saul H Rosenberg[1] & Steven W Elmore[1]

Proteins in the B cell CLL/lymphoma 2 (BCL-2) family are key regulators of the apoptotic process. This family comprises proapoptotic and prosurvival proteins, and shifting the balance toward the latter is an established mechanism whereby cancer cells evade apoptosis. The therapeutic potential of directly inhibiting prosurvival proteins was unveiled with the development of navitoclax, a selective inhibitor of both BCL-2 and BCL-2–like 1 (BCL-X_L), which has shown clinical efficacy in some BCL-2–dependent hematological cancers. However, concomitant on-target thrombocytopenia caused by BCL-X_L inhibition limits the efficacy achievable with this agent. Here we report the re-engineering of navitoclax to create a highly potent, orally bioavailable and BCL-2–selective inhibitor, ABT-199. This compound inhibits the growth of BCL-2–dependent tumors *in vivo* and spares human platelets. A single dose of ABT-199 in three patients with refractory chronic lymphocytic leukemia resulted in tumor lysis within 24 h. These data indicate that selective pharmacological inhibition of BCL-2 shows promise for the treatment of BCL-2–dependent hematological cancers.

Apoptosis, or programmed cell death, is a conserved and regulated process that is the primary mechanism for the removal of aged, damaged and unnecessary cells. The ability to block apoptotic signaling is a key hallmark of cancer and is thus important for oncogenesis, tumor maintenance and chemoresistance[1]. Dynamic binding interactions between prodeath (for example, BCL-2–associated X protein (BAX), BCL-2 antagonist/killer 1 (BAK), BCL-2–associated agonist of cell death (BAD), BCL-2–like 11 (BIM), NOXA and BCL-2 binding component 3 (PUMA)) and prosurvival (BCL-2, BCL-X_L, BCL-2–like 2 (BCL-W), myeloid cell leukemia sequence 1 (MCL-1) and BCL-2–related protein A1 (BFL-1)) proteins in the BCL-2 family control commitment to programmed cell death. Altering the balance among these opposing factions provides one means by which cancer cells undermine normal apoptosis and gain a survival advantage[2,3].

BCL-2, the first identified apoptotic regulator, was originally cloned from the breakpoint of a t(14;18) translocation present in human B cell lymphomas[2,4–6]. This protein has since been shown to have a dominant role in the survival of multiple lymphoid malignancies[7,8]. BCL-X_L was subsequently identified as a related prosurvival protein and is associated with drug resistance and disease progression of multiple solid-tumor and hematological malignancies[5,9,10]. We have previously established that BCL-X_L is also the primary survival factor in platelets[11,12]. Genetic ablation, hypomorphic mutation or pharmacologic inhibition of BCL-X_L results in reduced platelet half-life and dose-dependent thrombocytopenia *in vivo*[12].

The association of prosurvival BCL-2 family members with tumor initiation, disease progression and drug resistance makes them compelling targets for antitumor therapy[2]. Despite the fact that direct antagonism of proteins in the BCL-2 family requires disruption of protein-protein interactions, the use of structure-based drug design has recently rendered these proteins tractable targets[13]. We previously reported navitoclax (ABT-263), an orally bioavailable small molecule with a high affinity for both BCL-2 and BCL-X_L that is currently being evaluated in phase 2 clinical trials[14–18]. Both the antitumor efficacy and hematologic toxicities of navitoclax are dictated by its inhibition profile of prosurvival proteins in the BCL-2 family. Early signs of clinical antitumor activity have been observed in lymphoid malignancies thought to be dependent on BCL-2 for survival[16,17]. As predicted by preclinical data, inhibition of BCL-X_L by navitoclax induces a rapid, concentration-dependent decrease in the number

[1]AbbVie Inc., North Chicago, Illinois, USA. [2]Genentech, Inc., South San Francisco, California, USA. [3]The Walter and Eliza Hall Institute of Medical Research, Parkville, Victoria, Australia. [4]Faculty of Medicine, Dentistry and Health Sciences, University of Melbourne, Victoria, Australia. [5]Department of Clinical Hematology and Bone Marrow Transplantation, Royal Melbourne Hospital, Parkville, Victoria, Australia. [6]Department of Hematology, Peter MacCallum Cancer Centre, Melbourne, Victoria, Australia. [7]Present address: Division of Chemistry and Biological Chemistry, School of Physical and Mathematical Sciences, Nanyang Technological University, Singapore. Correspondence should be addressed to A.J.S. (andrew.souers@abbvie.com).

Received 17 July 2012; accepted 29 November 2012; published online 6 January 2013; doi:10.1038/nm.3048

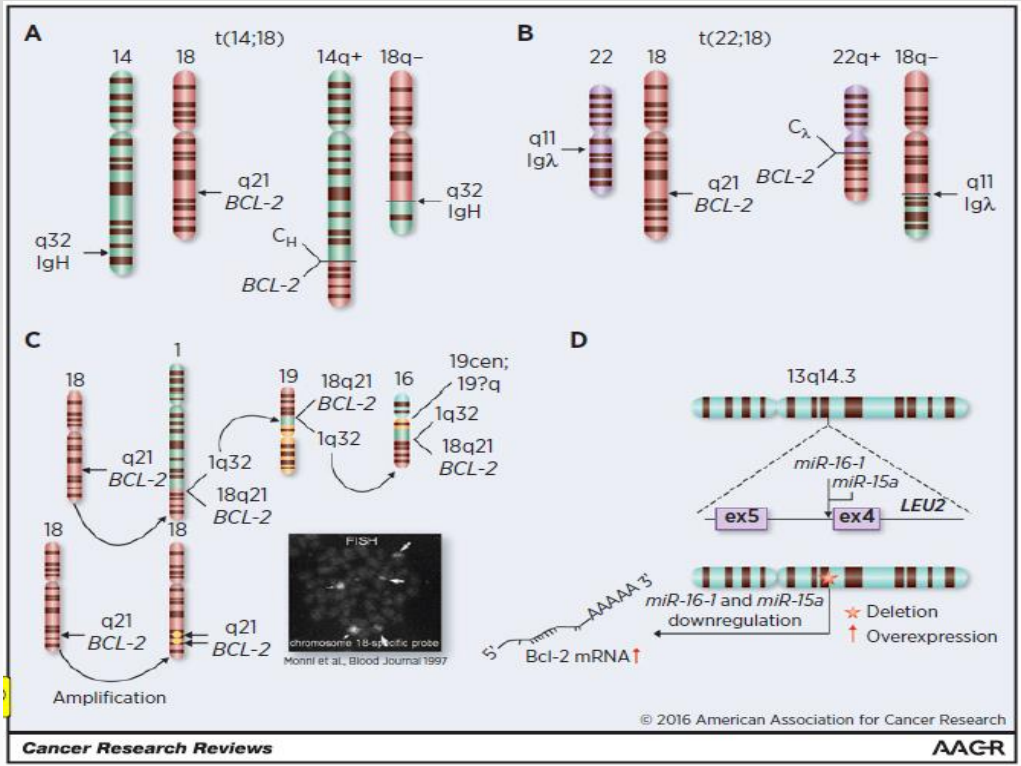

Figure 1.
Genetic lesions accounting for dysregulation of *BCL-2* gene expression in malignancies. **A,** the t(14;18) and the t(22;18) reciprocal chromosome translocations (**B**) are depicted. The translocations juxtapose the *BCL-2* gene to enhancer elements of the Ig loci causing deregulation of expression of *BCL-2*. **C,** *BCL-2* gene amplification schemes. Top, chromosome 18q–derived sequences are depicted with translocation to chromosome 1q32, which was further translocated to chromosomes 19 and 16. FISH using a chromosome 18-specific probe shows *BCL-2* amplification, three labels (large arrows) in addition to normal chromosomes (small arrows). Bottom,*BCL-2* gene amplification without chromosome rearrangements (**D**) The 13q14 genomic region is deleted in most CLLs. The genes encoding miR-15a and miR-16-1 lie within a 30-kb deleted region between exons 2 and 5 of the *DLEU2* gene. The deletion of miR-15a and miR-16-1 locus leads to Bcl-2 mRNA overexpression.

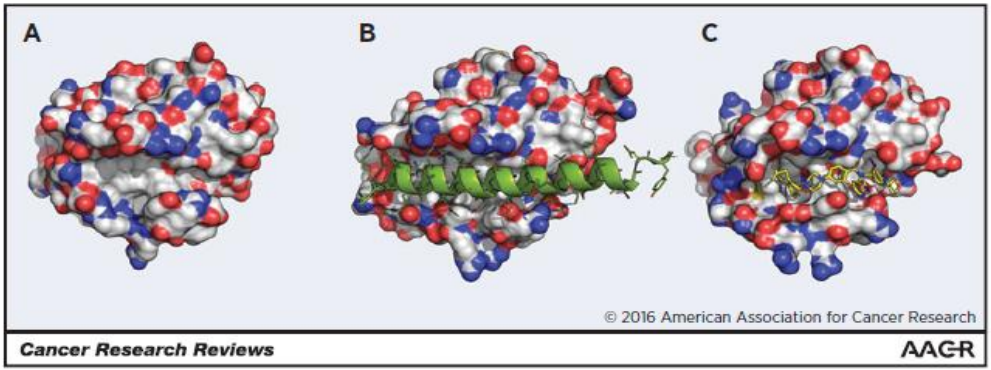

Figure 2.

Three-dimensional structure of antiapoptotic Bcl-2 family members. The 3D structure of the human Bcl-XL protein is depicted with an empty groove (**A**; PDB accession code: 1MAZ) and in complex with the BH3 peptide from Bim (**B**; PDB accession code: 1PQ1). The human Bcl-2 protein is represented in complex with a modeled structure of venetoclax based on the crystal structure of (4-(4-{[4-(4-chlorophenyl)-5,6-dihydro-2H-pyran-3-yl]methyl}piperazin-1-yl)-N-{[3-nitro-4-(tetrahydro-2H-pyran-4-ylamino)phenyl]sulfonyl}benzamide), a close analog (**C**; PDB accession code: 4MAN). The Connolly surface of the proteins is colored by mapped atom type (carbon, white; nitrogen, blue; oxygen, red; sulfur, yellow).

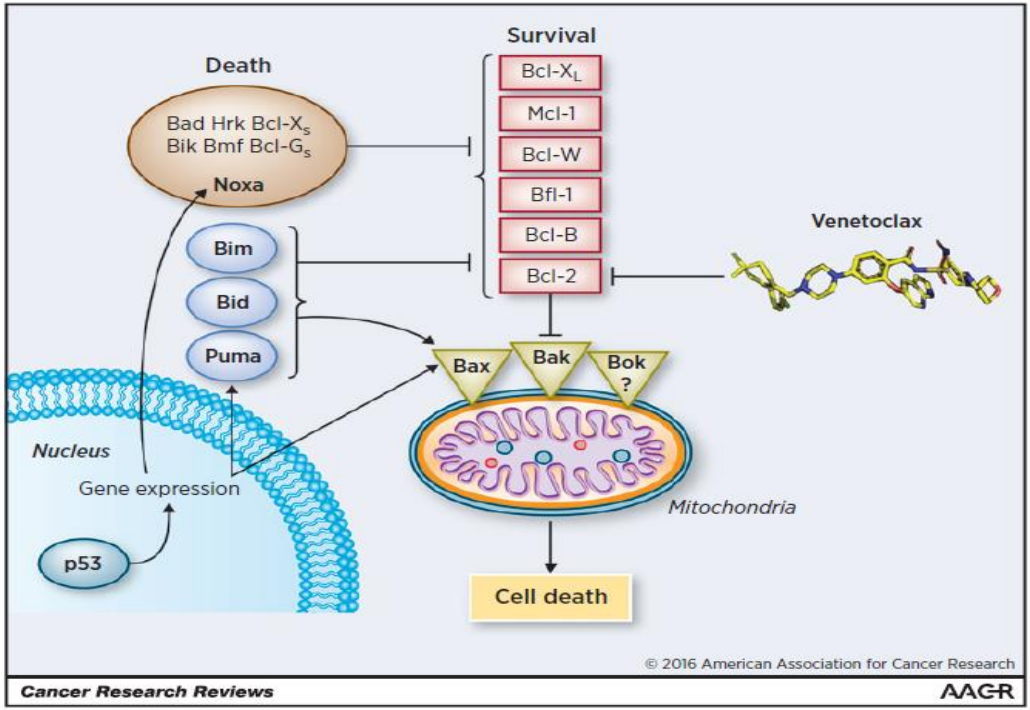

Figure 3.
Interactions among Bcl-2 family proteins. The categories of the Bcl-2 family are represented, including: (i) anti-apoptotic proteins, Bcl-2, Bcl-XL, Mcl-1, Bcl-W, Bfl-1, and Bcl-B (red); (ii) the multi-domain proapoptotic, Bax, Bak, and possibly Bok (yellow), which permeabilize the outer mitochondrial membrane; (iii) BH3-only proteins that operate as both agonists of proapoptotic Bax/Bak and antagonists of anti-apoptotic Bcl-2 members (pink); and (iv) BH3-containing proapoptotic members that operate as antagonists of the antiapoptotic proteins (orange). Tumor suppressor p53 plays important roles in responses to chemotherapy and stimulates transcription of specific proapoptotic members of the family (*BAX, PUMA, BID, NOXA*). Venetoclax is a selective antagonist of Bcl-2.

1984	14 ; 18 breakpoint cloned
1985-1986	Bcl-2 cDNA cloned ; sequenced
1988	Apoptosis suppression
1989	Bcl-2 poor progress in NHL
1990	Bcl-2 localized to mitochondria
1992	Chemoresistance
1993	Bax dimerizes with Bcl-2
1993	Bcl-2 over expressed in CLL
1993	ASO reverses chemoresistance
1994	Mitochondria required
1996	BH3 mediates dimerization
1996	Bcl-X 3D structure
1997	Bcl-2 ASO (Ph3 CLL)
1997	Bcl-XL + BH3 3D structure
1997	Bcl-2 gene amplified (DLBCL)
1999	SAR by NMR
2001	Bcl-2 3D structure
2002, 2005	MiR15-16 deletion (CLL)
2005	ABT 737 development
2007	Bcl-XL required for platelets
2007	Obatoclax discovered
2008	Navitoclax discovered
2009	Obatoclax Ph 1
2011	Navitoclax Ph 1
2013	Venetoclax discovered
2016	Venetoclax impressive activity in R/R CLL
2016	FDA approval

Gene Name	ROR1 low	ROR1 high	LINEAR FC	P value
hsa-miR-199a-5p	62.5	22.1	2.8	0.012
hsa-miR-451a	1653.0	610.4	2.7	0.006
hsa-miR-151a-3p	71.6	29.6	2.4	0.001
hsa-miR-151a-5p	131.6	55.1	2.4	0.001
hsa-miR-484	33.8	14.6	2.3	0.024
hsa-miR-132-3p	34.0	16.0	2.1	0.030
hsa-miR-199a-3p+hsa-miR-199b-3p	231.8	116.6	2.0	0.044
hsa-miR-15a-5p	2600.6	1327.4	2.0	0.006
hsa-miR-365a-3p+hsa-miR-365b-3p	105.9	59.7	1.8	0.043
hsa-miR-363-3p	183.1	107.1	1.7	0.005
hsa-miR-16-5p	18347.2	10848.8	1.7	0.003
hsa-miR-222-3p	1308.6	841.8	1.6	0.004
hsa-miR-337-3p	36.0	56.2	-1.6	0.028
hsa-miR-29a-3p	2011.4	3258.2	-1.6	0.002
hsa-miR-664a-3p	213.0	405.2	-1.9	<0.001
hsa-miR-148a-3p	411.8	1051.9	-2.6	0.009
hsa-miR-155-5p	1829.5	5064.8	-2.8	0.001

Tab. 1. Nanostring results

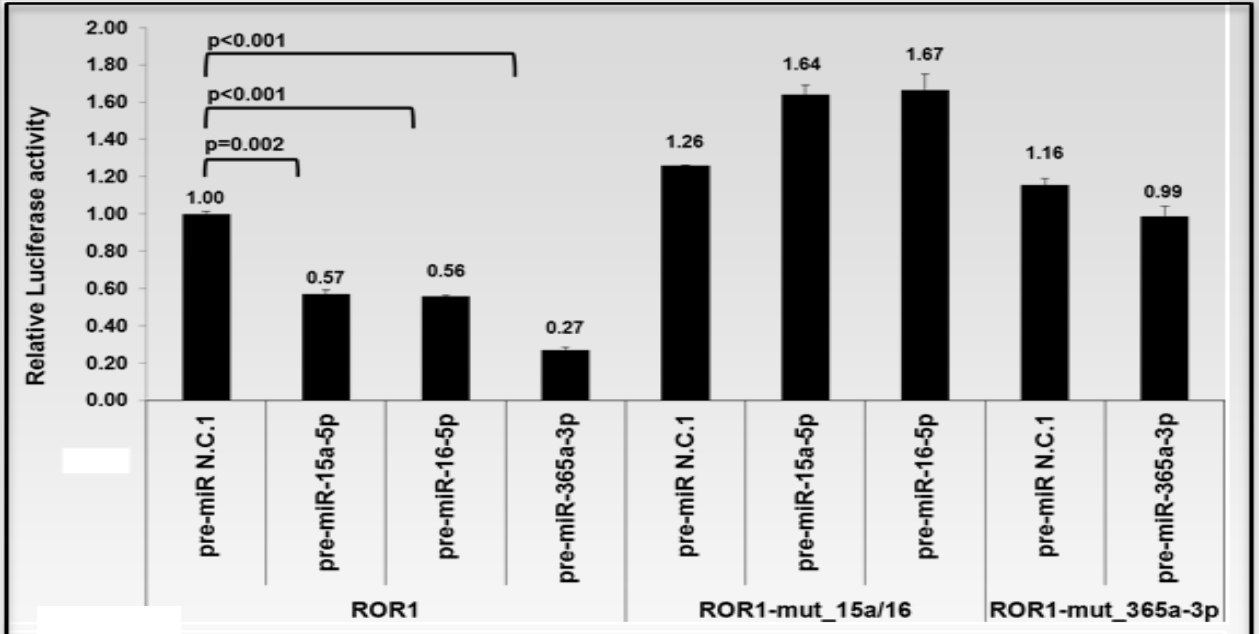

MiR15/16 targets ROR1 expression.

Transfection experiments were performed in HEK-293 cells using constructs indicated. First four lines show results using WT construct. Lines from 5 to 9 show results using constructs with mutant target sites.

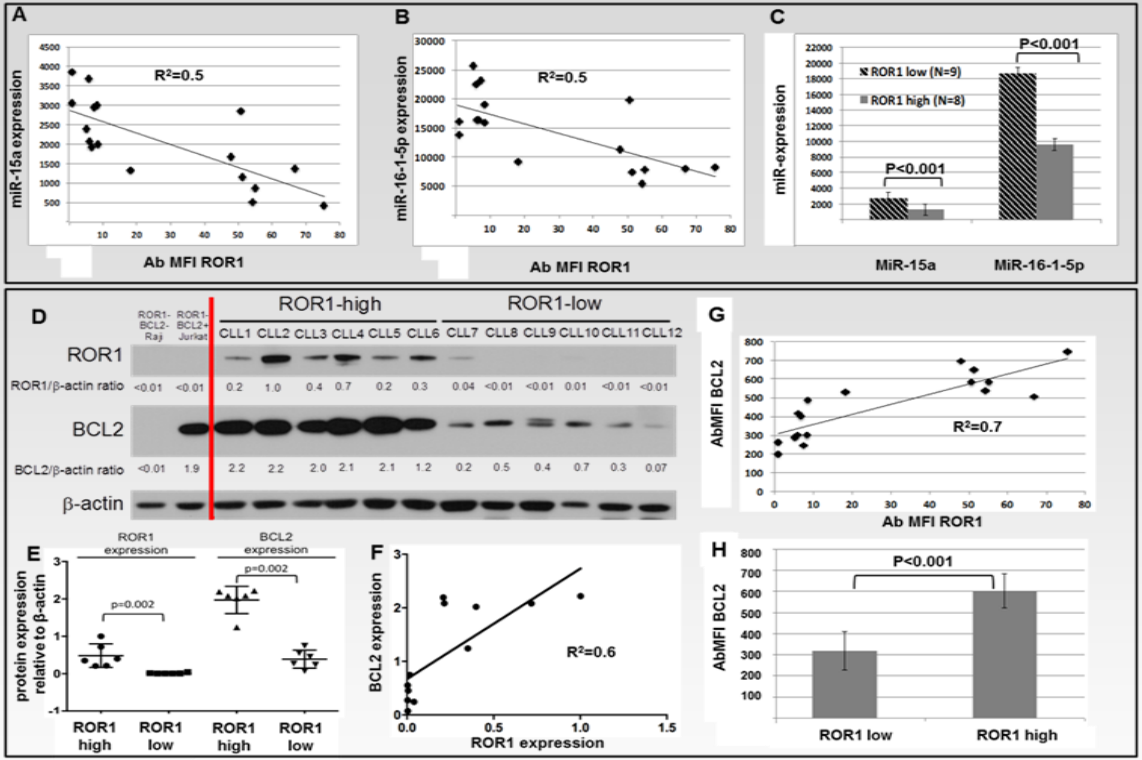

Fig. 4. Expression of miR15/16 ROR1 and BCL2 in CLL. A and B. Reverse correlation of miR15a and miR16-1-5p with ROR1 expression in CLL. C. Graphic representation of data in A and B. D. Correlation between BCL2 and ROR1 expression CLL. Jurkat cell were used as a positive control for BCL2 and Raji cells were used as negative control for BCL2. E. Densitometry analysis of data in D. The Mann Whitney U test was used to calculate p values. F. Correlation between BCL2 and ROR1 expression in CLL samples used in D. G. Correlation between BCL2 and ROR1 expression in CLL samples from the entire cohort A. The Absolute Median Fluorescence Intensity of intracellular BCL2 (AbMFI) is plotted on the Y axis and the AbMFI of surface ROR1 is charted on the X axis. H Graphic representation of data in G.

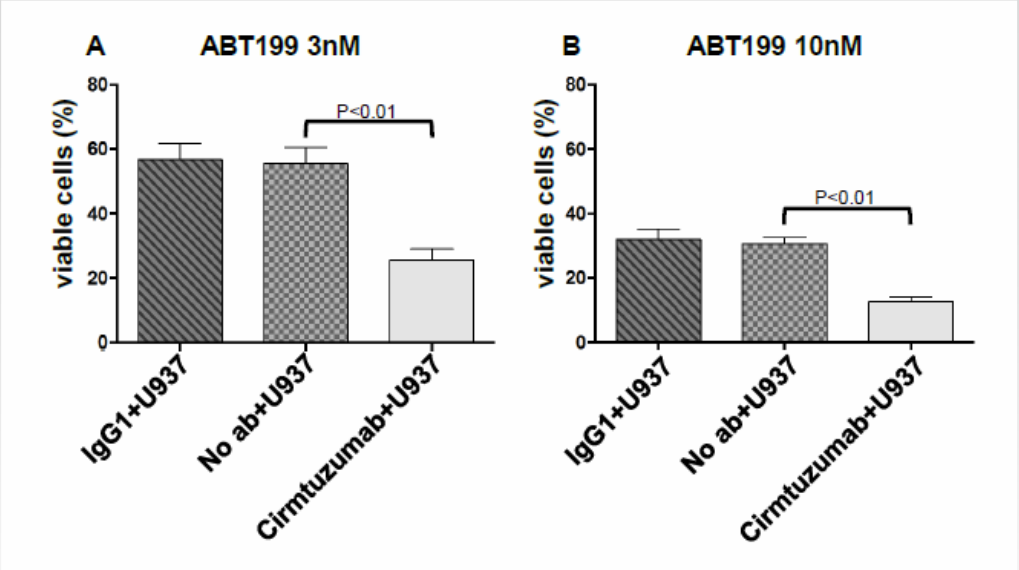

CLL cell viability with U937 effector cells. Bars indicate the average percentage of viable CLL cells normalized with respect to average percentage of viable untreated CLL cells. CLL cell viability is assessed after 16h treatment with 3 nM (**A**) or 10 nM (**B**) Venetoclax either alone or in combination with 20 mg/ml Cirmtuzumab or human IgG1 antibody. U937=human monocyte cell line, No Ab=no antibody control, Cirmtuzumab= anti human *ROR1* antibody, IgG1= anti human IgG1 antibody. Data are shown as mean ± s.e.m.

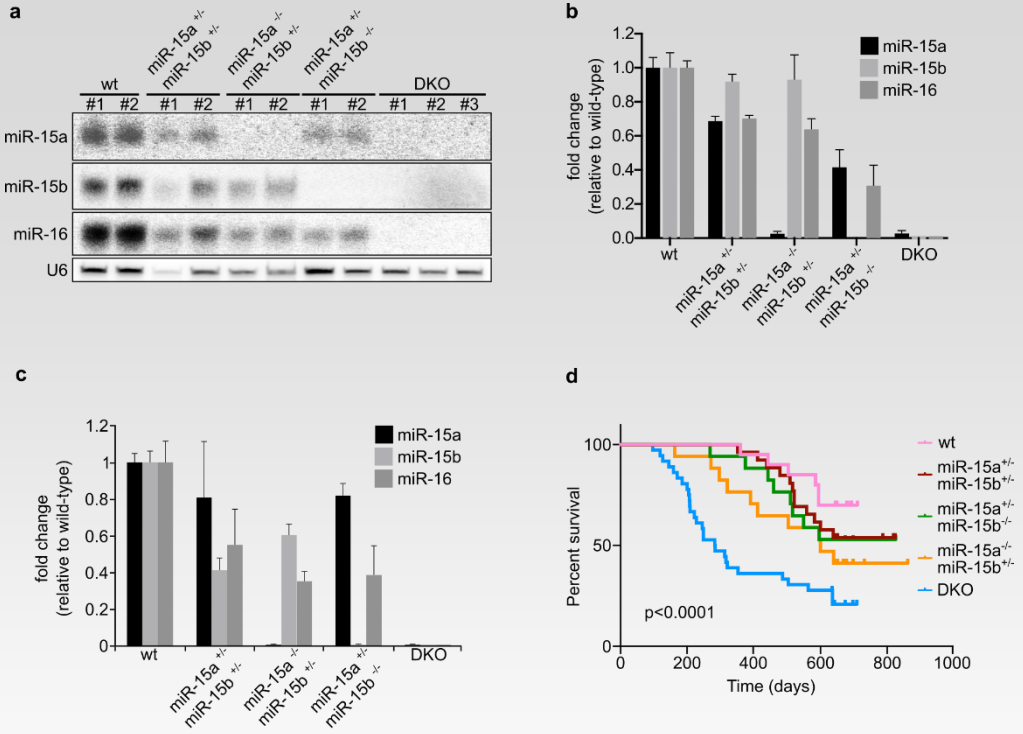

Deletion of miR-15/16 clusters in mice is associated to a shortened lifespan. a, Northern blot analysis of miR-15a, miR-15b and miR-16 in spleen from DKO mice compared to spleen from wild-type, heterozygous and single KO mice. Non-coding small nuclear RNA U6 was used as a loading control. **b**, Relative quantification of miR-15a, miR-15b and miR-16 expression respect to U6 loading control from Northern blot assay. **c,** qRT-PCR analysis of spleens from DKO mice compared to spleen from wild-type, heterozygous and single KO mice. Small nucleolar RNAs snoR-292 and snoR-135 were used for normalization. **d**, Survival curve of wild-type, heterozygous, single KO and DKO mice. Mice were followed for up to 24 months and events corresponded to mice that died to illness or those identified as moribund and then sacrificed (p value < 0.0001).

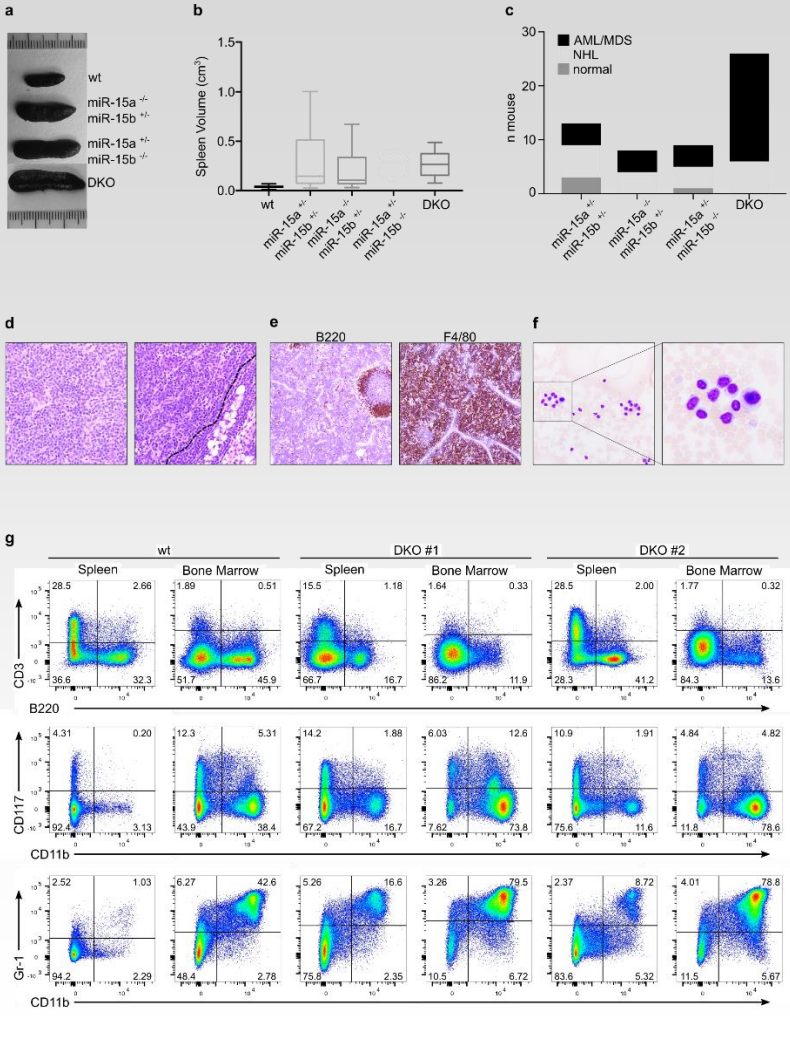

miR-15/16 DKO mice develop both myeloproliferative and lymphoproliferative diseases. a, Spleens from wild-type, single KO and DKO mice. **b,** Quantification of spleen volume (cm^3) of wild-type, single KO and DKO mice. T-test was used for statistical analysis. n.s indicates "not significant". *, $P \leq 0.05$; **, $P \leq 0.001$. **c,** Number of mice for each genotypes with myeloproliferative disorder and AML (AML/MDS) or with B-lymphoid pathologies (NHL) up to 24 month-old. **d,** Hematoxylin and eosin stain showing a small-to-medium neoplastic cell population destroying the spleen (left) and lymph node (right) normal architecture. **e,** B220 and F4/80 stained spleen sections from DKO mice confirmed the neoplastic expansion of a $B220^-$ and $F4/80^+$ cell lineage. **f,** Wright-Giemsa stained blood smear from DKO mouse showing clusters of blasts. **g,** Representative flow cytometry analysis of spleen and bone marrow of DKO and wild-type mice. CD3, B220, CD117, Cd11b and Gr-1 antibodies were used.

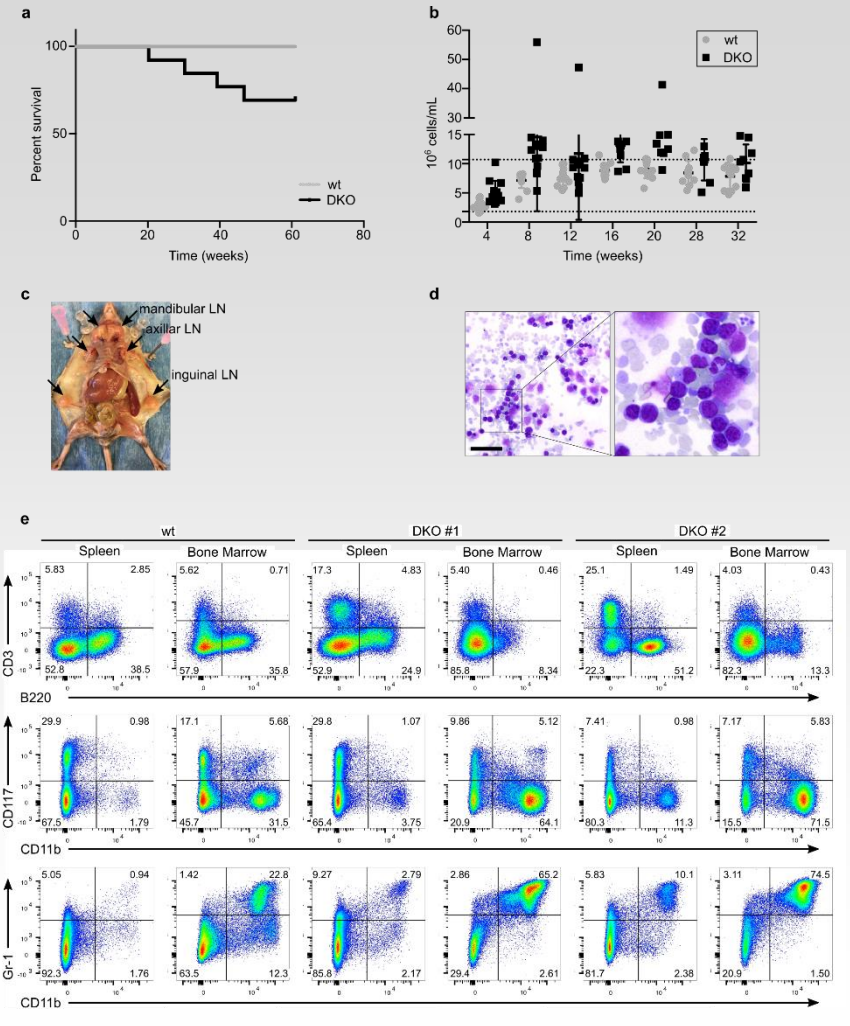

The transplant of miR-15/16 cluster DKO splenocytes results into the development of myeloproliferative disorders in recipient mice. a, Survival curve of wild-type and DKO recipient mice. Mice were followed for up to 32 weeks and events corresponded to mice that died to illness or those identified as sick and then sacrificed (*P* 0.05). **b,** White blood cells count using Hemavet instrument of wild-type and DKO mice. **c,** Representative of dissected DKO recipient mouse. Enlarged spleen and lymph nodes are highlighted. **d,** Wright-Giemsa stained blood smear from DKO recipient mouse showing clusters of blasts. **e,** Representative flow cytometry analysis of spleen and bone marrow of DKO and wild-type recipient mice. CD3, B220, CD117, Cd11b and Gr-1 antibodies were used.

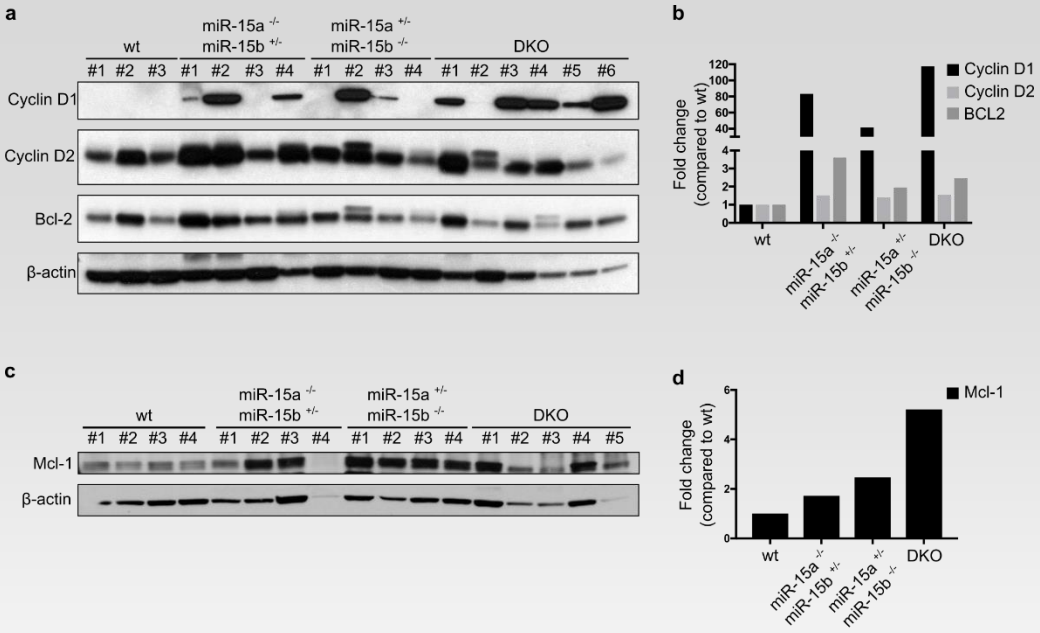

Validation of predicted targets of miR-15/16 cluster. a, Immunoblotting for Cyclin D1, Cyclin D2 and Bcl-2 performed on splenic cells lysates derived from wild-type and DKO mice. b-actin was used as a normalizer in order to show equal protein loading. **b,** Relative quantification of Cyclin D1, Cyclin D2 and Bcl-2 expression respect to b-actin loading control in splenic cells from DKO and wild-type mice. **c,** Immunoblotting for Mcl-1 performed on splenic cells lysates derived from wild-type and DKO mice. b-actin was used as a normalizer. **d,** Relative quantification of Mcl-1 expression respect to b-actin loading control.

mmu-miR-15a (chr14: 61632027-61632110)	5' UAGCAGCACAUAAUGGUUUGUG 3'
mmu-miR-15b (chr3: 69009772-69009835)	5' UAGCAGCACAUCAUGGUUUACA 3'
mmu-miR-16-1 (chr14: 61631880-61631972)	5' UAGCAGCACGUAAAUAUUGGCG 3'
mmu-miR-16-2 (chr3: 69009902-69009996)	5' UAGCAGCACGUAAAUAUUGGCG 3'

Table 2. Alignment of the mature sequences of the miR-15/16 family members. MiR-16-1 and miR-16-2 are identical.

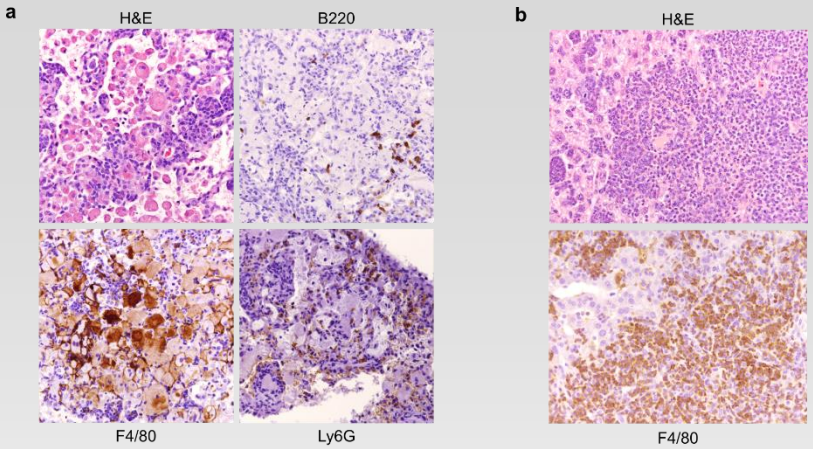

Extended Data Figure 1. a, Hematoxylin and eosin (top right), B220 (top left), F4/80 (bottom right) and Ly6G (bottom left) stained lung sections from DKO mice showing a F4/80^{+} large cell neoplastic infiltration resembling AML with maturation and megakariocytic differentiation. **b,** Hematoxylin and eosin (top row) and F4/80 (bottom row) stained liver sections from DKO mice showing a hepatic leukemic involvement.

Extended Data Figure 1

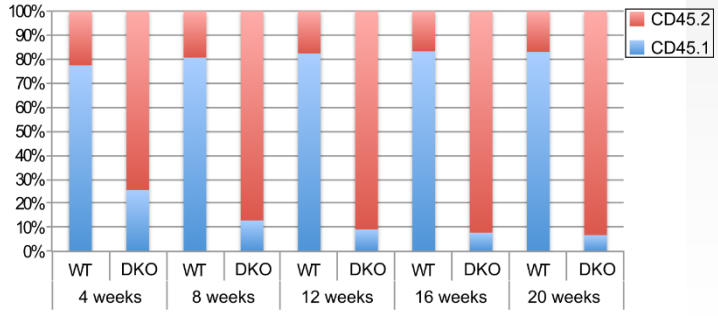

Extended Data Figure 2. Flow cytometry analysis of peripheral blood after transplantation using CD45.1 APC (donor cells) and CD45.2 PE (recipient/leukemic cells) antibodies at indicated time point.

Extended Data Figure 2

Characteristic	Value
Age at study entry – yr	57.67 ±17.15
Male sex – no. (%)	35 (50)
Initial white-cell count (Mean) (10^9/L)	76.35 ±84.15
Initial blasts count (Mean) (10^9/L)	52.73 ±69.94
Diagnosis – no. (%)	70 (100)
AML NPM1 mutated – no. (%)	23 (33)
AML with monocytic differentiation AND NPM1 mutated – no. (%)	1 (1)
AML with monocytic differentiation – no. (%)	3 (4)
AML with inv(16) – no. (%)	3 (4)
AML with inv(3) – no. (%)	2 (3)
AML with maturation – no. (%)	1 (1)
AML with minimal differentiation – no. (%)	1 (1)
AML with myelodysplastic related changes – no. (%)	13 (19)
AML with t(8;21) – no. (%)	1 (1)
AML with t(9;11) – no. (%)	1 (1)
AML without maturation – no. (%)	1 (1)
AML, NOS – no. (%)	12 (17)
Other subtype – no. (%)	8 (11)

Table 3. Characteristics of the AML patients included in the study

	Sample ID	Gender	Age of Dx	Diagnosis	Initial WBC (10^9/L)	Initial blast (10^9/L)	Cytogenetics	Molecular	Pt status
1	4306	Female	54	AML, NOS	47	39.25	46,XX [20]	NPM1 neg, FLT3-ITD neg	Alive
2	7625	Male	34	AML with t(8;21)	33.8	16.9	46,XY,t(8;21)(q22;q22),del(9)(q13q22)[9]/46,XY[1]	RUNX1/RUNX1T1 pos, KITneg	Alive
3	150375	Male	65	AML with NPM1 mutation	20	4.54	46,XY[10]	NPM1 pos, FLT3-ITD pos, FLT3-TKD neg	Deceased
4	150381	Female	59	AML with NPM1 mutation	31.9	3.51	46,XX [20]	NPM1 pos, FLT3-ITD neg, FLT3-TKD neg	Alive
5	150549	Female	56	AML	66.4	61.09	46,XX [20]	NPM1 neg, FLT3-ITD neg, FLT3-TKD neg	Deceased
6	150625	Female	32	AML with inv(3)	61.1	36	45,XX,inv(3)(q21q26.2),-7[11]/46,XX[1]	not done	Deceased
7	150718	Male	57	AML NPM1 mutated	152	136.8	46,XY[20]	NPM1 pos, FLT3-ITD pos, FLT3-TKD neg	Deceased
8	150749	Male	62	AML with myelodysplastic related changes	83.5	24.88	46,XY,del(5)(q22q31)[20]	not done	Deceased
9	150935	Male	21	AML with inv(16)(p13;q22)	92.3	71.99	46,XY,inv(16)(p13.1q22)[5]/46,XY[5]	CBFB-MYH11 pos, KIT neg	Alive
10	151011	Male	77	AML, NOS	5.3	1.08	47,XY,+8[18]/46,XY[2]	not done	Deceased
11	151044	Male	69	AML with NPM1 mutation	182.7	171.19	47,XY,+8[3]/46,XY[17]	NPM1 pos, FLT3-ITD pos, FLT3-TKD neg	Deceased
12	151050	Female	79	AML with NPM1 mutation	72.9	63.42	46,XX [20]	NPM1 pos, FLT3-ITD neg, FLT3-TKD pos	Deceased
13	151077	Male	77	AML with myelodysplastic related changes	167	147.29	46,XY,-7,+mar[5]/46,XY[2]	not done	Deceased
14	151149	Male	69	AML, NOS	71.9	68.02	46,XY[20]	NPM1 neg, FLT3-ITD pos, FLT3-TKD neg	Deceased
15	151156	Male	78	AML with inv(3)(q21q26.2)	21.7	13.15	44~45,X,-Y,del(2)(p17q21),inv(3)(q21q26.2),del(5)(q13q33),-7,-13,add(15)(q24),add(17)(p11.2),add(17)(p13),del(20)(q11.2),-21,add(21)(p11.2),-22,+2~4mar[cp10]	not done	Deceased
16	151311	Female	77	AML with monocytic differentiation	165	115.5	46,XX,del(5)(q13q31)[6]/47,idem,+11[14]	NPM1 pos, FLT3-ITD pos, FLT3-TKD neg	Deceased
17	151341	Female	78	Therapy-related AML	61.3	34.02	46,XX[20]	NPM1 neg, FLT3-ITD neg, FLT3-TKD neg	Deceased
18	151344	Male	66	AML with myelodysplastic related changes	37.1	13	46,XY,add(5)(p13),der(10)t(10;11)(p11.2;q13),del(11)(q23),del(12)(p11.2p13)[10]	NPM1 neg, FLT3-ITD neg, FLT3-TKD neg	Deceased
19	151566	Female	42	AML with mutated NPM1	112.5	95.06	46,XX[20]	NPM1 pos, FLT3-ITD neg, FLT3-TKD pos	Deceased
20	151598	Female	51	AML with mutated NPM1	21.6	12.7	46,XX [20]	NPM1 pos, FLT3-ITD neg, FLT3-TKD neg	Alive
21	160028	Female	22	AML, NOS	32.5	6.1	46,XX[16]	NPM1 neg, FLT3-ITD neg, FLT3-TKD neg	Alive
22	160053	Female	37	AML, NPM1 mutated	326	305	unsuccessful	NPM1 pos, FLT3-ITD neg, FLT3-TKD neg	Alive
23	160114	Male	70	AML with monocytic differentiation	123.5	80.77	46,XY[20]	NPM1 neg, FLT3-ITD pos, FLT3-TKD neg	Deceased
24	160142	Female	65	AML with inv (16)	70.9	36.09	INV (16) AND inv(16)(p13.1q22)	CBFB-MYH11 pos, KIT neg	Alive
25	160326	Male	67	AML with myelodysplastic related changes	36.7	23.67	45,X,-Y,-9,add(17)(p11.1),+mar1[4]/45,X,-Y,-9,-17,+20,+mar1[2]/45,X,-Y,+1,der(1;17)(q10;q10)[2]/46,XY[4]	not done	Deceased
26	160345	Male	68	AML with mutated NPM1	11.1	1.23	46,XY[20]	NPM1 pos, FLT3-ITD pos, FLT3-TKD neg	Deceased
27	160414	Male	77	Therapy-related AML	24.1	2.82	46,XY,-10,der(16)t(10;16)(q22;p13.3),+mar[7]/46,XY,del(7)(q22),t(10;16)(q22;p13.3)[3]	not done	Deceased
28	160601	Male	75	AML with mutated NPM1	22.6	6.74	46,XY[20]	NPM1 pos, FLT3-ITD pos	Alive
29	160757	Female	61	AML with NPM1 mutation	118.4	111.41	46,XX [20]	NPM1 pos, FLT3-ITD neg	Alive
30	160846	Male	28	AML with mutated NPM1	107.5	81.38	unsuccessful	NPM1 pos, FLT3-ITD neg, FLT3-TKD pos	Alive
31	160906	Female	63	AML with myelodysplastic related changes	142.3	125.76	46,XX,del(9)(q13q22)[11]	NPM1 neg, FLT3-ITD pos, FLT3-TKD neg	Deceased
32	160950	Female	68	AML with myelodysplastic related changes	1	0.05	46,XX [20]	NPM1 neg, FLT3 TKD neg, FLT3 ITD neg, PML/RARA neg	Deceased
33	161072	Male	46	AML with inv(16)(p13.1q22)	51.7	30.5	47,XY,+8,inv(16)(p13.1q22)[8]/48,sl,+22[2]	KIT pos, CBFB-MYH11 pos	Alive
34	161102	Female	62	AML	44	5.28	46,XX,del(5)(q13q31)[5]/46,XX[2]	not done	Alive
35	161153	Female	68	AML with myelodysplastic related changes	328.7	65.74	46,XX [20]	NPM1 neg, FLT3-ITD pos	Deceased
36	161172	Male	34	AML without maturation	135.4	120.64	46,XY,del(3)(q12q25)[9]/46,XY[1]	NPM1 neg, FLT3-ITD neg	Alive
37	161200	Male	62	AML with NPM1 mutation	117.1	60.89	46,XY[20]	NPM1 pos, FLT3-ITD neg	Deceased
38	161210	Female	69	AML with maturation	60.4	41.5	46,XX,t(7;9)(q32;q12)[2]/47,XX,+19[2]/46,XX[16]	not done	Alive
39	161216	Female	83	AML with NPM1 mutation	26.1	17.2	46,XX,der(4)t(3;4)(q12;q35)[7]/46,XX,dup(3)(q12q29)[2]	NPM1 pos, FLT3-ITD neg	Deceased
40	161240	Female	50	AML	22.1	6.85	46,XX[20]	not done	Deceased
41	161254	Female	66	AML with myelodysplastic related changes	12.6	9.72	44~50,XX,-5,del(5)(q13q33),-7,-10,+11,add(12)(p11.2),+14,+15,add(19)(q13.4),	not done	Deceased
42	161282	Male	38	AML, NOS	18.1	14.34	46,XY,del(9)(q13q22)[2]/46,XY[18]	NPM1 neg, FLT3-ITD neg	Alive
43	161305	Male	47	AML, NOS	133.5	123.09	48,XY,t(6;11)(q27;q23),+21,+21[20]	NPM1 neg, FLT3-ITD neg	Deceased
44	161380	Female	66	AML with NPM1 mutation	377.8	361.56	unsuccessful	NPM1 pos, FLT3-ITD pos	Alive
45	161406	Male	66	AML, NOS	11.4	6.84	46,XY[20]	NPM1 neg, FLT3-ITD neg	Deceased
46	161407	Female	67	AML with mutated NPM1	34.2	23.74	46,XX [20]	NPM1 pos, FLT3-ITD neg	Deceased
47	161421	Female	59	AML with NPM1 mutation	316	205.4	unsuccessful	NPM1 pos, FLT3-ITD pos	Alive
48	161498	Female	57	AML	29.3	21.01	46,XX [20]	NPM1 neg, FLT3-ITD neg, CBFB-MYH11 neg	Alive
49	161528	Female	49	AML, NOS	14.5	9.28	46,XX,t(11;19)(q23;p13.1)[13]/46,XX[7]	PML/RARA neg	Alive
50	161660	Female	74	AML with mutated NPM1	40.5	29.69	46,XX[20]	NPM1 pos, FLT3-ITD neg	Deceased
51	161673	Female	77	AML with myelodysplastic related changes	5.7	0.51	46,XX[18]	NPM1 neg, FLT3-ITD neg	Deceased
52	161734	Male	48	AML with mutated NPM1	59.5	53.85	47,XY,+13[6]/46,XY[4]	NPM1 pos, FLT3-ITD neg	Alive
53	161769	Male	68	AML with minimal differentiation	26.9	16.01	unsuccessful	NPM1 neg, FLT3-ITD neg	Deceased
54	161780	Male	19	AML, NOS	40.1	36.49	46,XY,t(10;11)(p12;q23)[10]	not done	Deceased
55	161820	Male	30	AML with t(9;11)(p22;q23)	179	27.39	47,XY,+X,t(9;11)(p22;q23)[10]	not done	Deceased
56	161868	Male	63	AML with mutated NPM1	85.2	55.64	46,XY[20]	NPM1 pos, FLT3-ITD pos	Deceased
57	161905	Male	67	AML with myelodysplastic related changes	16.9	13.99	43,XY,del(5)(?q11.2q35),add(7)(q36),add(13)(p11.2),-15,-17,-17,-18,der(20)t(15;20)(q11.2;q13.1),	not done	Deceased
58	162002	Female	70	AML with myelodysplastic related changes	28.1	16.59	46,XX[20]	NPM1 neg, FLT3-ITD pos	Deceased
59	162089	Male	38	AML, NOS	136.4	113.21	46,XY,del(9)(q13q22)[7]/47,idem,+8[2]/46,XY[1]	not done	Deceased
60	162102	Female	54	AML with monocytic differentiation	12.3	10.7	46,XX,idic[7](q11.1)[10]	not done	Alive
61	162111	Male	18	AML with mutated NPM1	40.8	22.8	45,X,-Y[9]/46,XY[11]	NPM1 pos, FLT3-ITD neg, CBFB-MYH11 neg	Alive
62	162131	Female	64	AML with myelodysplastic related changes	57.4	10.45	46,XX[20]	NPM1 neg, FLT3-ITD pos	Alive
63	162218	Male	70	AML, NOS	24.3	18.95	unsuccessful	NPM1 neg, FLT3-ITD pos	Deceased
64	162229	Female	64	AML, NOS	17.1	7.25	48,XX,+13,+13[9]/46,XX[2]	NPM1 neg, FLT3-ITD neg	Deceased
65	162235	Female	59	AML with NPM1 mutation	34.4	22.02	46,XX[20]	NPM1 pos, FLT3-ITD neg	Alive
66	162252	Female	25	AML with NPM1 mutation	48	43.2	46,XX[20]	NPM1 pos, FLT3-ITD neg	Alive
67	162292	Female	70	Therapy-related AML	105.6	73.92	46,XX,del(1)(p22p32),t(8;21)(q22;q22)[9]/46,XX[2]	KIT neg,RUNX1/RUNX1T1 pos	Deceased
68	162335	Male	68	AML with monocytic differentiation	30	6.8	46,XY[20]	NPM1 neg, FLT3-ITD neg	Alive
69	162372	Male	23	AML	8.9	5.6	45,X,-Y[20]	RUNX1/RUNX1T1 pos, KIT pos	Alive
70	166054	Male	73	AML with myelodysplastic related changes	18.8	17.33	47,XY,+11[10]/47,XY,+8[2]	NPM1 neg, FLT3-ITD neg	Deceased

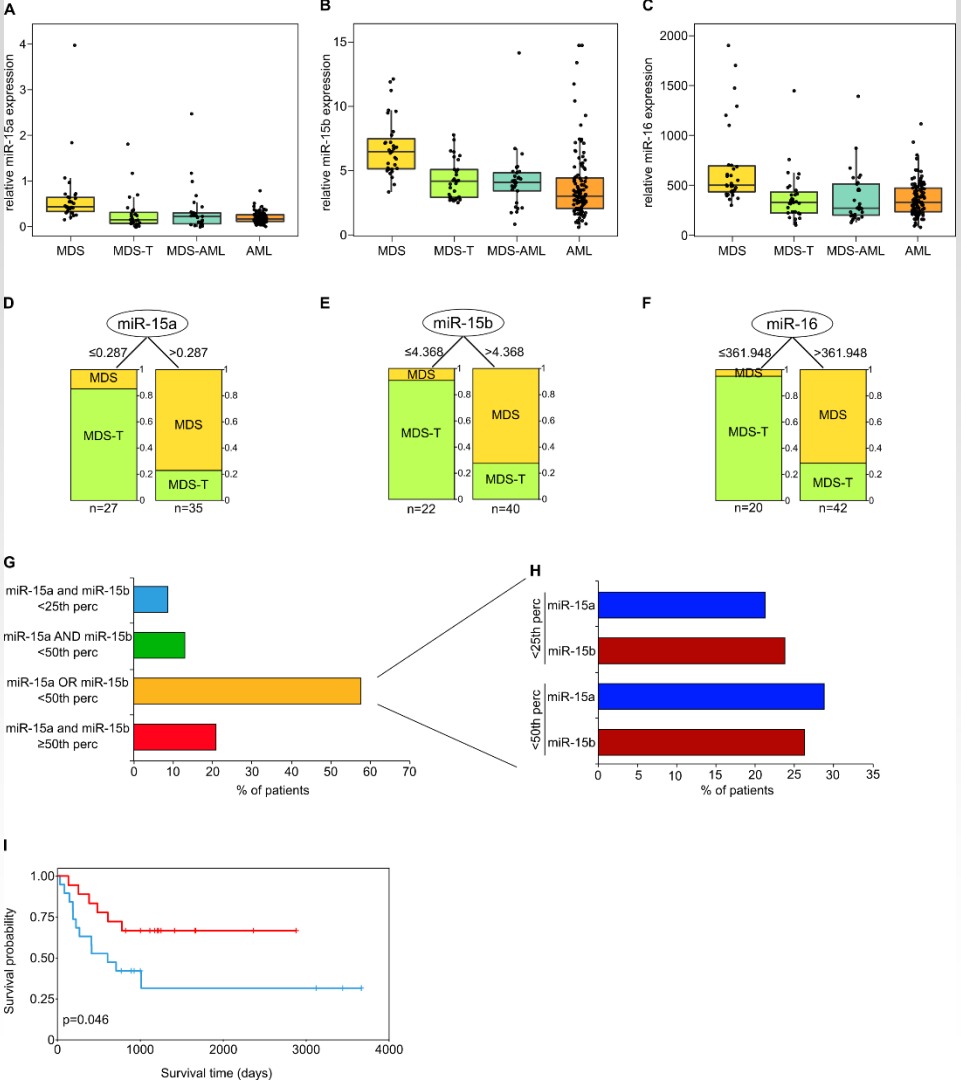
A
relative miR-15a expression
MDS
MDS-T
MDS-AML
AML
B
relative miR-15b expression
C
relative miR-16 expression
D
miR-15a
≤0.287
>0.287
n=27
n=35
E
miR-15b
≤4.368
>4.368
n=22
n=40
F
miR-16
≤361.948
>361.948
n=20
n=42
G
miR-15a and miR-15b <25th perc
miR-15a AND miR-15b <50th perc
miR-15a OR miR-15b <50th perc
miR-15a and miR-15b ≥50th perc
% of patients
H
<25th perc
<50th perc
miR-15a
miR-15b
% of patients
I
Survival probability
p=0.046
Survival time (days)

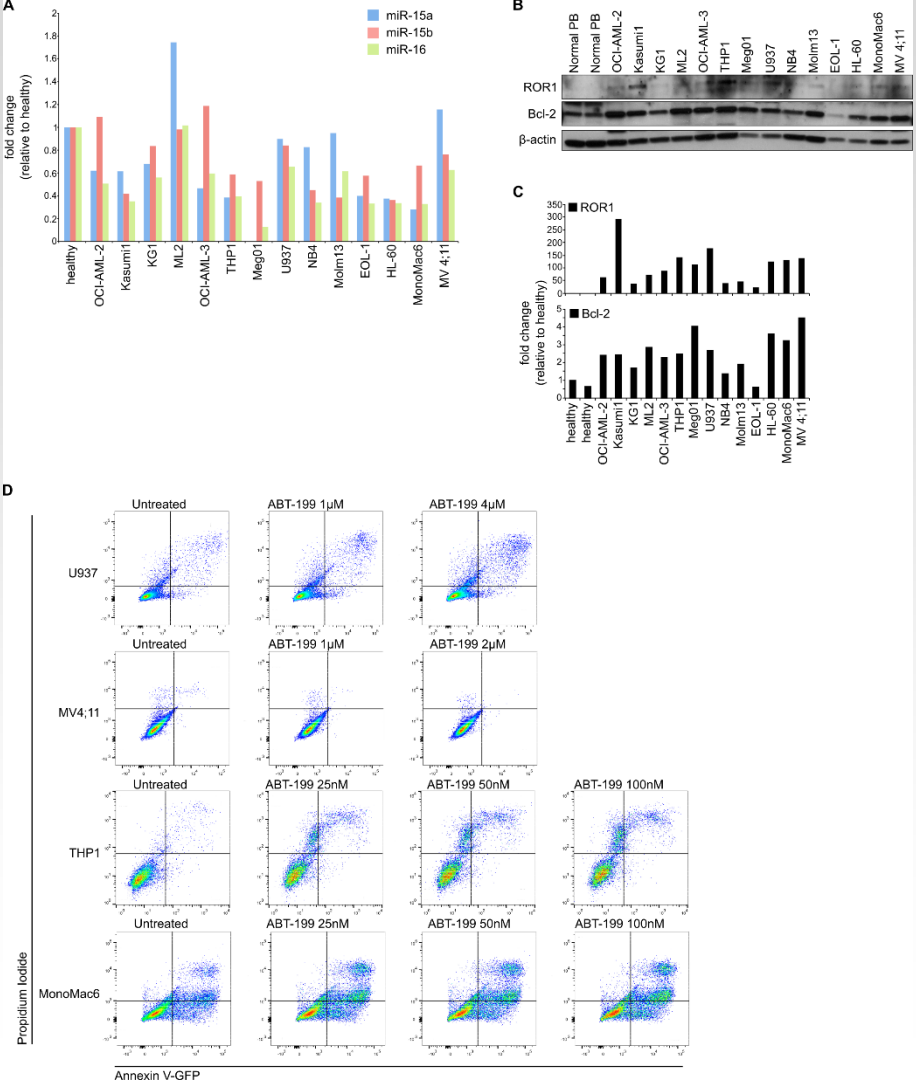
A
miR-15a
miR-15b
miR-16
fold change (relative to healthy)
healthy
OCI-AML-2
Kasumi1
KG1
ML2
OCI-AML-3
THP1
Meg01
U937
NB4
Molm13
EOL-1
HL-60
MonoMac6
MV 4;11
B
Normal PB
Normal PB
OCI-AML-2
Kasumi1
KG1
ML2
OCI-AML-3
THP1
Meg01
U937
NB4
Molm13
EOL-1
HL-60
MonoMac6
MV 4;11
ROR1
Bcl-2
β-actin
C
ROR1
Bcl-2
fold change (relative to healthy)
D
Untreated
ABT-199 1μM
ABT-199 4μM
U937
Untreated
ABT-199 1μM
ABT-199 2μM
MV4;11
Untreated
ABT-199 25nM
ABT-199 50nM
ABT-199 100nM
THP1
Untreated
ABT-199 25nM
ABT-199 50nM
ABT-199 100nM
MonoMac6
Propidium Iodide
Annexin V-GFP

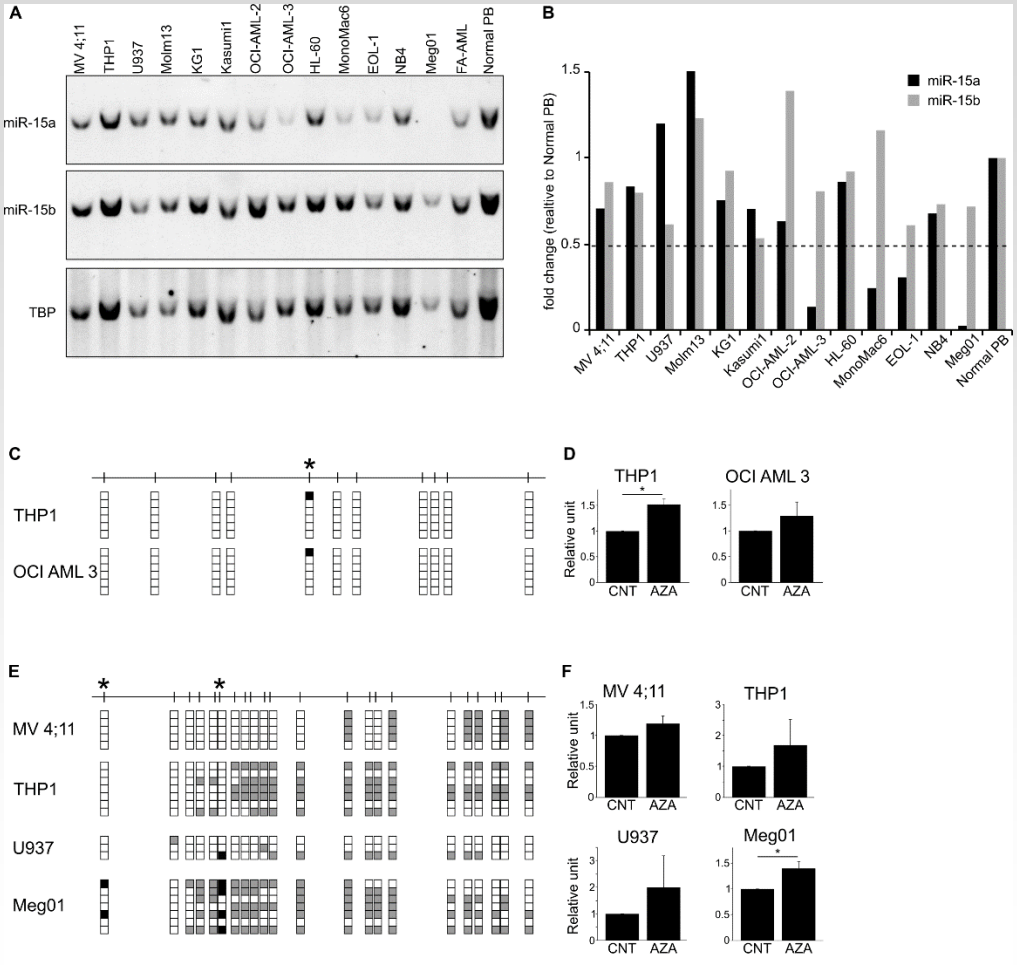
A
MV 4;11
THP1
U937
Molm13
KG1
Kasumi1
OCI-AML-2
OCI-AML-3
HL-60
MonoMac6
EOL-1
NB4
Meg01
FA-AML
Normal PB
miR-15a
miR-15b
TBP
B
miR-15a
miR-15b
fold change (realitive to Normal PB)
1.5
1
0.5
0
MV 4;11
THP1
U937
Molm13
KG1
Kasumi1
OCI-AML-2
OCI-AML-3
HL-60
MonoMac6
EOL-1
NB4
Meg01
Normal PB
C
THP1
OCI AML 3
D
THP1
OCI AML 3
Relative unit
CNT
AZA
E
MV 4;11
THP1
U937
Meg01
F
MV 4;11
THP1
U937
Meg01
Relative unit
CNT
AZA